THE JOURNAL OF PHYSICAL CHEMISTRY B

Article

pubs.acs.org/JPCB

Entropy Contribution toward Micelle-Driven Deintercalation of Drug−DNA Complex

Animesh Patra,[†,§] Soumitra Hazra,[‡,§] Gopinatha Suresh Kumar,*[,‡] and Rajib Kumar Mitra*[,†]

[†]Unit for Nano Science & Technology Department of Chemical Biological and Macromolecular Sciences S.N. Bose National Centre for Basic Sciences Block JD, Sector III, Salt Lake, Kolkata 700098, INDIA

[‡]Biophysical Chemistry Laboratory Chemistry Division CSIR- Indian Institute of Chemical Biology 4, Raja S.C. Mullick Road, Kolkata 700032, INDIA

Supporting Information

ABSTRACT: Micelle-assisted "deintercalation" of intercalated drug/mutagen molecules from DNA is a well-established phenomenon; however, the driving energy cost for such a process is still not properly understood. In the present contribution, we have estimated the various energetic parameters for the SDS micelle-assisted deintercalation of a model DNA intercalator phenosafranine (PSF) using isothermal titration calorimetry (ITC) measurement. Both steady-state and picosecond-resolved fluorescence measurements provide strong evidence for the relocation of PSF molecules from the DNA interior to the micellar interface at an SDS concentration above cmc. The overall deintercalation process has been found to be enthalpy-wise forbidden (endothermic); however, it is strongly favored by a high positive entropy change, which can be correlated with the change in the associated hydration structure at the macromolecular interface.

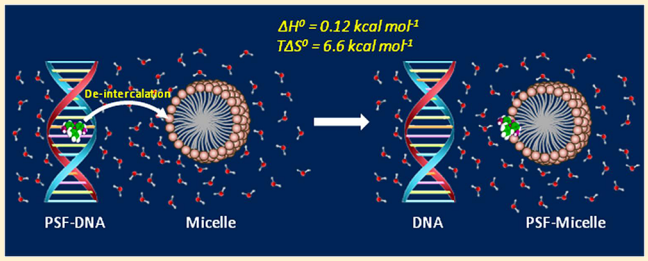

INTRODUCTION

Studies on the interaction of small molecules (ligands or drugs or mutagens) with DNA and correlating those to biological effects have been the focus of interest in science for many years.[1,2] A detailed understanding of the mechanism of how small drug (or mutagen) molecules recognize and reversibly bind to DNA is a prerequisite of a rational drug design. The formation and dissociation process of drug−DNA complexes provide useful information on DNA delivery into cells through membrane fusion and/or endocytosis. It remains necessary to obtain information on the structures of drug−DNA complexes, the dynamics of complex formation, and the energetics that drives the process. The drug−DNA interaction is believed to proceed in three successive steps: (1) a conformational change in DNA to accommodate the drug, (2) hydrophobic transfer of the drug into the site and (3) establishment of noncovalent $\pi-\pi$ staking interaction between the drug and the DNA interior in order to anchor the drug.[2,3] Two broad classes of noncovalent DNA binding interactions have been identified, the intercalation and the minor groove binding. In the former one, intercalators bind by inserting a planar aromatic chromophore between adjacent DNA pairs, whereas in the later one, the binders fit into the DNA minor groove. Detailed thermodynamic studies have suggested that a large hydrophobic contribution is responsible for the binding free energy of intercalation;[2,4,5] however, there is evidence of a large negative enthalpy contribution opposed by a unfavorable entropy term to facilitate the intercalation process.[6] Hydration also plays a key role in binding affinity and specificity of drug interaction with DNA.[7−9] Systematic investigation by the group of Chaires et al.[10,11] has revealed that the intercalation process involving the common intercalators is associated with an uptake of 6−30 water molecules upon complexation. These results strongly conclude that addition or release of water from the DNA surface plays an important role in the intercalation process.

The surface of DNA can often be realized in the form of charged micelles, which can be configured as a spherical polyelectrolyte, with a charged exterior and a hydrophobic interior. The formation and structure of charged micelles have been studied in depth,[12,13] and it has been inferred that a gain in entropy energetically favors the formation of micelles. Several experimental and simulation studies have revealed that water molecules present at the surface of micelles are bound to the surface and show properties different from bulk water.[14−17] It therefore can serve as a model system to understand the intercalation properties of drug into DNA and more importantly the hydrophobic transfer step that involves the equilibrium between the intercalator and the macromolecules.[6,18] Intercalation studies of a model drug daunomycin into SDS and TX-100 micelles have revealed that the binding affinity of the drug to the micelles is only slightly less than that with DNA; however, in contrast to the DNA binding, the binding with the micelles is associated with a favorable entropic contribution,[6] which infers that the binding needs to be considered in a more

Received: September 13, 2013
Revised: January 4, 2014
Published: January 8, 2014

complex manner, possibly as a combination of classical[12,19] and nonclassical[20,21] hydrophobic effects. In this context, it is interesting to study the micelle-induced "deintercalation" phenomenon[22−26] in which the presence of micelles extract the intercalated drug/mutagen out of the DNA interior and place it in the micelles. It has been believed that micelles modulate the drug−DNA binding equilibrium and provide a hydrophobic sink for the drug. The detergent sequestration technique is a well-known phenomenon,[27,28] and micelles are supposed to assist the dissociation of DNA-bound drug by absorbing the free dissociated drugs and thereby shifting the equilibrium toward deintercalation without disturbing the DNA structure. A detailed kinetic study by Westerlund et al.[22] shows that the rate of dissociation of cationic DNA-binding ligands increases markedly in the presence of surfactant molecules in monomeric as well as in micellar forms. The rate-enhancing effect depends upon the hydrophobic chain length of the surfactants. Such a deintercalation phenomenon has significant prospect in many biological processes; however, a detailed investigation on the driving force of the process is still lacking. A proper understanding of the deintercalation process needs a systematic thermodynamic approach, which would offer a substantial input toward specific therapeutic applications as surfactant molecules are present in real biological systems (e.g., in the form of phospholipids in the cell membrane). In the present contribution, we have investigated the energetics of the deintercalation process of a well-known DNA intercalator phenosafranine (PSF; 3,7-diamino-5-phenylphenazinium chloride),[29−31] which can act as a model drug, against a hydrophobic sink of SDS micelles using the isothermal titration calorimetry (ITC) technique. The intercalation process has been investigated using both a steady-state and a picosecond-resolved fluorescence spectroscopic technique. Our principle focus is to initiate a preliminary study in order to understand the energetic cost that drives a deintercalation process.

MATERIALS AND METHODS

Calf thymus (CT) DNA, phenosafranine (PSF, Scheme 1), and sodium dodecyl sulfate (SDS) were purchased from Sigma

Scheme 1. Molecular Structure of Phenosafranine (PSF)

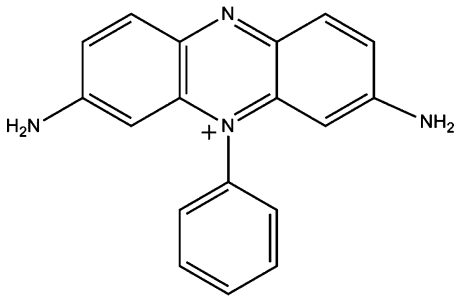

Aldrich Corporation and used without further purification. The phosphate salts (sodium monophosphate and biphosphate) were obtained from SRL (India) and were used as received. The stock solution of DNA was prepared by dissolving solid DNA in a 10 mM phosphate buffer (pH∼7). Freshly prepared DNA solutions were used for all the experiments. The concentration of DNA was determined spectrophotometrically using the molar extinction coefficient ε_{DNA} = 6600 M^{-1} cm^{-1} at 260 nm.[31] The purity of DNA was verified by monitoring the absorbance ratio $A_{260\ nm}/A_{280\ nm}$, which was always found to be in the range of 1.8−1.9. PSF solution was prepared in the experimental buffer solutions. The concentration of PSF solution was determined using its molar extinction coefficient, ε = 33 000 M^{-1} cm^{-1} in water (measured at 521 nm).[32] Circular dichroism (CD) measurements were performed in a JASCO J815 spectrometer using 1 cm path length cuvettes. All the experiments were carried out at 25 °C.

Steady-state absorption and fluorescence measurements were carried out using a Shimadzu UV-2450 spectrophotometer and a Jobin Yvon Fluorolog-3 fluorimeter, respectively. All the steady-state emission spectra of PSF were collected at an excitation wavelength of 510 nm. The steady-state anisotropy (r) was obtained by measuring the fluorescence intensities with the excitation polarizer oriented vertically and the emission polarizer oriented vertically (I_{VV}) and horizontally (I_{HV}), respectively, according to the following relation, $r = ((I_{VV} - GI_{HV})/(I_{VV} + 2GI_{HV}))$. The grating factor ($G$) is obtained as $G = (I_{HV})/(I_{HH})$. Time-resolved fluorescence measurements were performed on a commercially available spectrophotometer (LifeSpec-ps) from Edinburgh Instruments, Ltd., U.K. (excitation wavelength 445 nm, 80 ps instrument response function (IRF)). Fluorescence transients were fitted by using software F900 from Edinburgh Instruments. The details of the time-resolved measurements can be found elsewhere.[15] The time-dependent fluorescence Stokes shifts, as estimated from TRES (time-resolved emission spectra), were used to construct the normalized spectral shift correlation function or the solvent correlation function, $C(t)$, defined as

$$C(t) = \frac{\nu(t) - \nu(\infty)}{\nu(o) - \nu(\infty)} \quad (1)$$

where, $\nu(0)$, $\nu(t)$, and $\nu(\infty)$ are the emission maximum frequency (in cm^{-1}) at time zero, t, and infinity. The $\nu(\infty)$ values are the emission frequency at a time where we find no more changes. The $C(t)$ function represents the temporal response of the solvent relaxation process, as occurs around the probe following its photoexcitation and the associated change in the dipole moment. For time-resolved rotational anisotropy ($r(t)$) measurements, emission polarization was adjusted to be parallel or perpendicular to that of the excitation, and anisotropy is defined as

$$r(t) = \frac{I_{para} - GI_{per}}{I_{para} + 2GI_{per}} \quad (2)$$

where G is the grating factor determined following a long-time tail-matching technique.[32]

Isothermal titration calorimetry (ITC) was performed on a MicroCal VP-ITC unit (MicroCal, Inc., Northampton, MA), at 25 °C, after electrical and chemical calibrations. PSF, DNA, and SDS solutions were degassed on the MicroCal's Thermovac unit prior to loading in order to avoid the formation of bubbles in the calorimeter cell. Aliquots (10 μL for each injection) of degassed SDS solution were injected from a rotating syringe (311 rpm) into the isothermal sample chamber containing each of the solutions [1.42 mL, 300 μM PSF and PSF−DNA (1:20) complex titrated with 60 mM SDS]. Corresponding control experiments to determine the heat of dilution for SDS were performed by injecting identical volumes of the same concentration of SDS into the buffer. The duration of each injection was 10 s, and the interval between each injection was 240 or 300 s. The initial delay before the first injection was 60 s. Each injection generated a heat burst curve (μcal s^{-1} vs time).

dx.doi.org/10.1021/jp4091816 | J. Phys. Chem. B 2014, 118, 901−908

The area under each heat burst curve was determined by integration using the Origin 7.0 software (MicroCal) to give the measure of the heat associated with that injection. The heat associated with each SDS-buffer mixing was subtracted from the corresponding heat associated with the SDS injection to the PSF or PSF/DNA complex to give the heat of the reaction. The resulting corrected injection heats were plotted as a function of the molar ratio of [PSF/SDS], fit with a model for one set of binding sites, and analyzed using Origin software to estimate the association constant (K_b) and the enthalpy of binding (ΔH^o). The Gibbs energies (ΔG^o) and entropic contribution to the binding ($T\Delta S^o$) were calculated using the standard relationship

$$\Delta G^0 = -RT\ln K_b = \Delta H^0 - T\Delta S^0 \quad (3)$$

RESULTS AND DISCUSSION

Figure 1 (inset) depicts the steady-state emission spectra of PSF (excited at 510 nm) in the presence of different concentrations

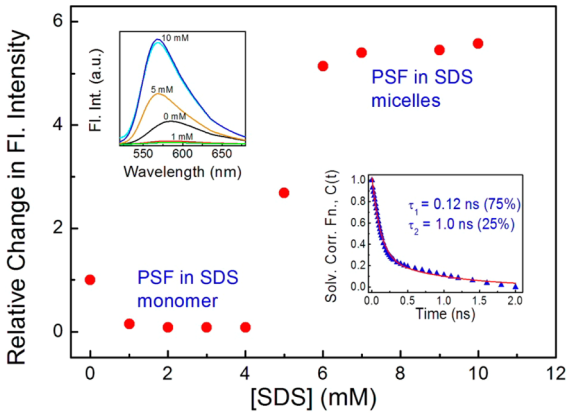

Figure 1. Relative change in fluorescence intensity of PSF as a function of SDS concentration. Corresponding emission spectra are shown in the inset. Solvent correlation function, $C(t)$ of PSF in SDS micelles is shown in the other inset. Solid line represents biexponential fit.

of SDS. PSF in buffer produces an emission peak at ~585 nm, which suffers a progressive blue shift with increasing SDS concentration to produce a peak at ~570 nm in the SDS micellar region. We plot the relative change in fluorescence intensity of the dye as a function of SDS concentration (Figure 1). The relative intensity initially drops (at low SDS concentration) and a many-fold enhancement of fluorescence intensity is observed as the cmc_{SDS} is approached (the cmc of SDS is ~8 mM, which reduces to 4.6 mM in presence of 10 mM phosphate buffer.[33]) The initial decrease of the fluorescence is due to the quenching of the PSF emission by SDS at low concentration, as has previously been observed in the case of a similar cationic dye (nile blue)−SDS system[25] The observed quenching had been explained in terms of the formation of dye−surfactant ion pairs which progressively associate to form an aggregated like structure.[34] The many-fold increase in the emission intensity at higher SDS concentration clearly suggests a strong binding of the drug with the micelles, a phenomenon much anticipated keeping in mind the overall positive charge of PSF and negative surface charge of SDS micelles.[31,35] However, the binding location of the drug in the micelle is a point of concern here. As we consider the oppositely charged drug molecule, it is certain that PSF prefers to reside in the outer Stern layer of the micelle rather than placing itself into the Palisade layer or deep inside the micellar core, resulting in a considerable exposure of the drug toward the aqueous environment. In order to understand the nature of hydration as well as the relaxation dynamics of the drug in aqueous and micellar environments, we carry out time-resolved fluorescence measurements. The average lifetime of the drug in water is found to be ~1.0 ns, which increases to ~1.95 ns in micellar environment (data not shown). From the wavelength-dependent decay transients of PSF in the micellar environment, we construct the time-resolved emission spectra (TRES) (Figure S1, Supporting Information). Using the TRES data, we determine the time-resolved solvent correlation function, $C(t)$, and it is fitted biexponentially with the corresponding time constants of 0.12 ns (75%) and 1.0 ns (25%) (Figure 1, inset).

The obtained time constants are retarded an order of magnitude compared to the sub picosecond relaxation time constant of bulk water[36] and signifies a considerable interaction of the drug with the micellar interface. However, it is interesting to note here that we observe a very marginal time-resolved Stokes shift of ~50 cm^{-1}, which is merely ~4% of the observed steady-state Stokes shift. The limitation of the instrumental response time (IRF~80 ps) refrains us from recovering the ultrafast fluorescence signal coming from bulk water. In a previous study,[15] we recovered ~40% of the fluorescence signal with a hydrophobic drug 4-(dicyanomethylene)-2-methyl-6(*p*-dimethylamino-styryl) 4*H*-pyran (DCM) embodied in the hydrophobic layer of SDS micelles. Thus, the limited recovery of the fluorescence signal in the present investigation affirms the effluent aqueous exposure of PSF in SDS micelle. In order to understand the geometrical restriction imposed to the drug by the micellar environment, we measure the time-resolved rotational anisotropy of PSF in micellar environment (Figure S2, Supporting Information). The observed anisotropy decay is fitted biexponentially with time constants of 0.12 (27%) and 1.06 ns (73%). The faster component resembles the time constant of PSF in bulk water,[31] which re-establishes the exposure of the drug in the aqueous environment, whereas the slower component signifies the interaction of the drug with the micellar surface.

The fluorescence profile of PSF−DNA interaction has been depicted in Figure 2. Increasing the concentration of DNA quenches the PSF emission; the intensity drops first rapidly and then gradually, a behavior much consistent with another cationic drug (Nile Blue)−DNA interaction.[25,26] The initial

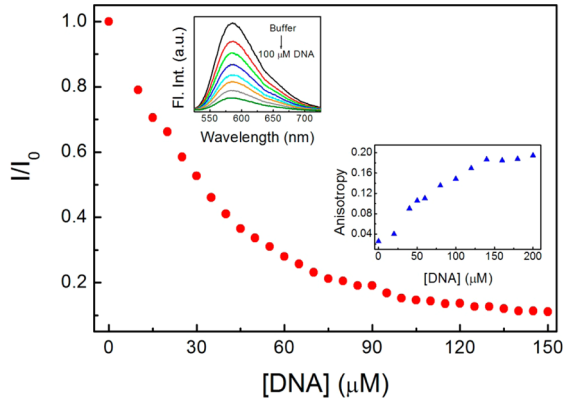

Figure 2. Quenching of PSF fluorescence in the presence of DNA. Inset shows the corresponding emission spectra. Steady-state anisotropy of PSF has been shown in the other inset as a function of the DNA concentration.

dx.doi.org/10.1021/jp4091816 | J. Phys. Chem. B 2014, 118, 901−908

binding of a cationic dye with the DNA surface is essentially electrostatic in nature, which produces the primary quenching;[37,38] at higher DNA concentrations, the drug intercalates and quenching occurs through electron transfer.[39] We have measured the steady-state anisotropy of PSF in the presence of DNA (Figure 2, inset), and it is found that anisotropy increases first rapidly and then steadily to reach a plateau. The increased anisotropy is associated with a restricted motion of the drug as it binds to the DNA and at a concentration ~15 times higher than that of PSF the anisotropy then reaches a plateau, clearly signifying the onset of the formation of the DNA–PSF intercalated complex.[29,30,40,41] The highly quenched DNA intercalated PSF emission provides a very low photon count during the time-resolved measurements to extract any meaningful information.

The deintercalation phenomenon is observed spectrophotometrically (Figure 3) as SDS is added to an intercalated

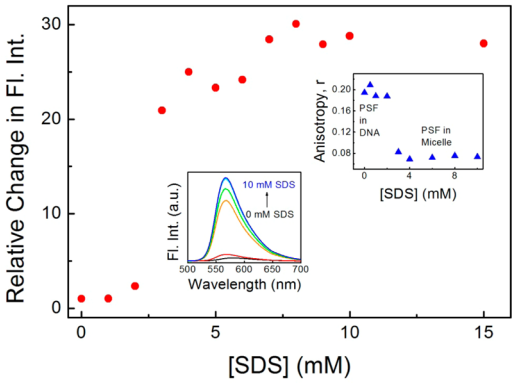

Figure 3. Relative changes in fluorescence intensity of the PSF–DNA complex. Corresponding emission spectra are shown in the inset. Steady-state anisotropy of PSF intercalated to DNA in the presence of different concentrations of SDS is shown in the other inset.

PSF–DNA complex (with a stoichiometric ratio of 1:20, which ensures complete intercalation). As can be observed from Figure 3, there occurs a considerable (~10 nm) blue shift of the emission maximum coupled with a many-fold increase in the fluorescence intensity beyond cmc_{SDS}. The emission maximum obtained at ~570 nm in presence of a high SDS concentration strongly corresponds to that of PSF in the micellar environment (see Figure 1), which clearly identifies that the drug relocates itself from DNA environment to the micellar environment. To further verify this conclusion, we measured the steady-state anisotropy of the intercalated drug–DNA complex in presence of SDS (Figure 3).

The high steady-state anisotropy (r~0.2) of the drug–DNA complex undergoes a sharp decrease beyond cmc_{SDS} and reaches a value comparable to that in SDS micelles (~0.07),[31] and the observed fall in anisotropy is in exact confirmation of the relocation of the drug in the micellar interface. Time-resolved anisotropy measurements also provide a similar conclusion, as the rotational anisotropy time constants match in excellent agreement to that obtained for the SDS–PSF complex (figure not shown). The complete deintercalation can further be confirmed by monitoring the induced circular dichroism (CD) spectra of PSF–DNA complex in the spectral region of 450–650 nm (Figure S3, SI). A strong positive CD band (~555 nm) and a week negative band (~505 nm) develop during the intercalation of PSF into the DNA. The induced CD spectra are generated due to the asymmetric arrangement of the bound PSF molecules in the DNA helix.[29] The positive ellipticity band increases with increasing DNA concentration, keeping a fixed concentration of PSF (50 μM), and ultimately reaches saturation. When SDS is added to the intercalated PSF–DNA (1:20) complex, the positive band decreases with increasing SDS concentration and eventually disappears, implying a complete deintercalation of the drug.

In this regard, it is pertinent to understand the role of hydration change during the intercalation process. The osmotic stress method provides an easy estimate to the change in the hydration during drug–DNA intercalation.[42,43] We estimate the binding constant of PSF–DNA in the presence of different concentrations of sucrose using the following model: because addition of DNA quenches the emission of PSF, the concentration of free drug is obtained as $C_f = C_t(((F/F_0) - P)/(1 - P))$, where F is the observed emission intensity under a particular set of DNA and PSF concentrations, F_0 is the emission intensity at the same PSF concentration in absence of DNA, and P is the ratio of the completely bound to free drug, $P = (F_b)/(F_0)$.[44] The amount of bound drug is determined by the difference, $C_b = C_t - C_f$. The total concentration of the drug (C_t) is determined as $C_t = (A_{520})/(\varepsilon_{520})$ (molar extinction coefficient (ε) of PSF is 33 000 M^{-1} cm^{-1} at 520 nm and A is the measured absorbance). The binding ratio (r) is defined as, $r = (C_b)/([DNA]_{total})$. Binding data obtained from spectrofluorimetric titrations are cast into a Scathered plot of r/C_f versus r (Figure 4

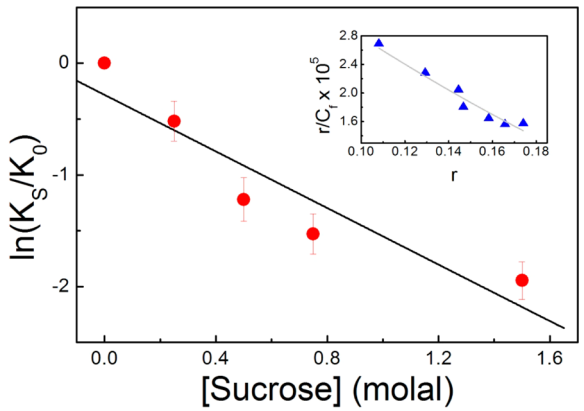

Figure 4. Natural logarithm of the ratio of the binding constant at a given sucrose concentration (K_s) relative to the binding constant in buffer (K_0) is shown as a function of solution osmolality. Solid line represents linear fit. Inset shows Scatchard plot from fluorescence emission data for the binding of PSF-DNA. Solid line in the inset represents the nonlinear least-squares fit of the experimental points to the McGhee–von Hippel equation.

inset). Scatchered plots are then fitted assuming a non-cooperative binding using the following equation developed by McGhee and Von Hippel[45]

$$\frac{r}{C_f} = K_i(1 - nr)\left[\frac{1 - nr}{1 - (n - 1)r}\right]^{(n-1)} \quad (4)$$

where K_i is the intrinsic binding constant to an isolated binding site and 'n' is the number of base pairs excluded by the binding of a single drug molecule. The binding affinity is observed to decrease with increasing osmolyte concentration, a phenomenon comparable to the other intercalators.[10] The change in hydration (Δn_w) can be obtained using the relation

dx.doi.org/10.1021/jp4091816 | J. Phys. Chem. B 2014, 118, 901–908

$$\frac{\partial \ln(K_s/K_0)}{\partial[\text{osm}]} = -\left(\frac{\Delta n_w}{55.5}\right) \quad (5)$$

and a linear fit (Figure 4) provides an estimate of ~70 ± 16 water molecule uptake during the intercalation process. A positive Δn_w value (uptake of water) might appear surprising at first glance; however, it may be noted that Δn_w is the difference in the number of bound water molecules between the complex and the free reactants. Crystallographic studies have revealed a considerable number of apparently specifically bound water molecules in a ligand–DNA complex,[46] which are otherwise not present in their individual hydrated form. It can also be noted that for intercalators which possess additional subunits that can interact with the minor groove of DNA, an additional layer of bound water can form. These effects eventually produce a positive Δn_w value as had been observed for other intercalators.[10,11]

The energetic parameters of the micelle-assisted PSF deintercalation are studied by isothermal titration calorimetry (ITC). Figure 5 depicts representative ITC profile diagrams

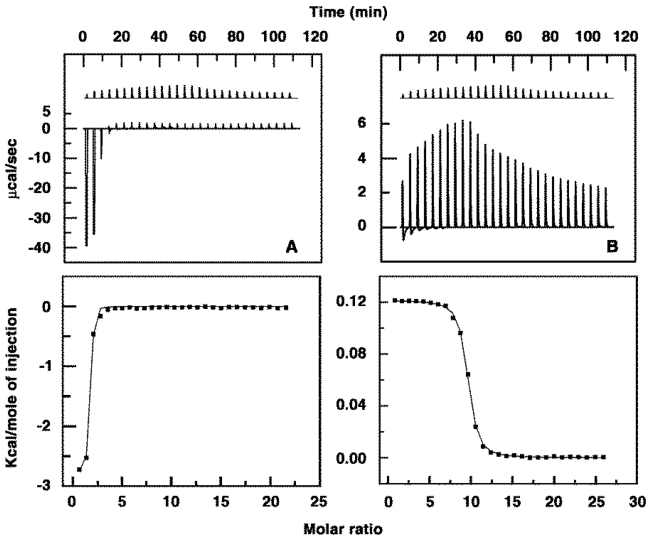

Figure 5. Representative ITC profiles for the titration of PSF (A) and the PSF/DNA (1:20) complex (B) with SDS. Top panels represent the raw data for sequential injection of SDS into PSF and the PSF/DNA complex, and bottom panels show the integrated heat data after correction of heat of dilution against the molar ratio of PSF/SDS. Data points are fitted to the one-site model, and the solid lines represent the best-fit data. Top panel, upper curve is the dilution of SDS into phosphate buffer (not in scale) at pH ~ 7.0.

of the titration of PSF and PSF–DNA complex with SDS. The ITC profile diagram of the titration of PSF with DNA is shown in Figure S4 (Supporting Information). Thermodynamic parameters obtained from the ITC experiments are summarized in table 1. It can be observed that the intercalation of PSF into DNA is an exothermic process (ΔH^0 = −2.96 kcal mol^{-1}) associated with a large positive entropy contribution ($T\Delta S^0$ = 4.59 kcal mol^{-1}), resulting in an overall feasibility of the binding process (ΔG^0 = −7.55 kcal mol^{-1}) at 25 °C. The moderate negative enthalpy change for a "large" singly charged drug PSF can be interpreted as the dispersion of hydrogen bonds in the formation of cavity for the drug.[47] Apart from the polyelectrolyte contribution, the intercalative binding free energy (ΔG^0) of a drug into DNA could be deconvoluted into several contributions, namely,[2] conformational changes in DNA (ΔG_{conf}), loss of translational and rotational degrees of freedom (ΔG_{r+t}), hydrophobic transfer of the drug from bulk to the DNA (ΔG_{hyd}), and weak covalent bonds (ΔG_{mol}). While the first two terms add unfavorable contributions, the high negative value of the third term overwhelms to favor the binding process. For most of the intercalators, ΔG_{conf} contributes a share of +4 kcal mol^{-1},[4] while (ΔG_{r+t}) offers a considerable unfavorable contribution of ~15 kcal mol^{-1}. The ΔG_{hyd} has been reported to be −7.8 kcal mol^{-1} for PSF–DNA binding,[30] concluding a favorable ΔG_{mol} value of ~17 kcal mol^{-1} associated with the process, which is comparable to that obtained in other intercalators like ethidium and propidium, among other.[2]

The PSF–SDS binding is exothermic (ΔH^0 = −2.77 kcal mol^{-1}) with a high positive entropy change ($T\Delta S^0$ = 4.50 kcal mol^{-1}), both favoring the spontaneity of the binding process (ΔG^0 = −7.27 kcal mol^{-1}). The high positive entropic contribution and an overall exothermicity determines that the binding of PSF with SDS involves a possible disruption of the hydrogen-bonded water structure about the micellar surface, as has also been inferred in the spectroscopic investigation. Because PSF–DNA and PSF–SDS have comparable binding energetics, it is interesting to investigate what drives the deintercalation process. The ITC experiment reveals that addition of SDS micelles into a fully intercalated PSF–DNA (1:20) complex involves a small positive enthalpy change (ΔH^0 = 0.12 kcal mol^{-1}) with a large positive entropy contribution ($T\Delta S^0$ = 6.62 kcal mol^{-1}), making the overall deintercalation process energetically favorable (ΔG^0 = −6.49 kcal mol^{-1}) (Table 1).

The deintercalation process can be modeled as the sum of two independent steps

$$[\text{PSF–DNA}]_{hyd} \leftrightarrows \text{DNA}_{hyd} + \text{PSF}_{hyd} \quad \text{(Process I)}$$

$$[\text{SDSmicelle}]_{hyd} + \text{PSF}_{hyd} \rightarrow [\text{PSF–micelle}]_{hyd} \quad \text{(Process II)}$$

where all the species are in their respective hydrated forms in the aqueous solution. The model is a rather simplified one and assumes that any other transient steps associated with the two major processes either contribute a minor share or that their contributions are taken care of by the overall equilibrium thermodynamic parameters. Assuming that the binding process is reversible, the unbinding of PSF–DNA should offer an endothermic contribution ($\Delta H^0_{\text{Process I}} \sim 3$ kcal mol^{-1}). Because $\Delta H^0_{\text{Process II}} \sim -2.8$ kcal mol^{-1}, an overall unfavorable endothermic contribution of ~0.2 kcal mol^{-1} can be estimated. This value is in excellent agreement with that obtained in the ITC experiment (Table 1), which supports the assumption that Process I and Process II occur successively. The overall feasibility (ΔG^0 = −6.49 kcal mol^{-1}) of the deintercalation process therefore receives significant contribution from the entropy change. The contributions from the monomeric hydration of PSF cancel out. Thus, one needs to consider the other four energy terms only. The total free energy change is a cumulative contribution of two broad interactions, namely, electrostatic interaction (ΔG^0_{el}) and nonpolar interaction (ΔG^0_{np}). The electrostatic term originates from the interactions between the various charged species present (i.e., PSF, micelle, and DNA). The total free energy due to these electrostatic interactions can be summarized as

$$\Delta G^0_{el} = \Delta G^0_{\text{DNA–PSF}} + \Delta G^0_{\text{micelle–PSF}} + \Delta G^0_{\text{DNA–micelle}} \quad (6)$$

Generally, the contribution of the nonpolar interaction is higher than the corresponding electrostatic contribution,[48] which,

dx.doi.org/10.1021/jp4091816 | J. Phys. Chem. B 2014, 118, 901–908

Table 1. Thermodynamic Parameters Derived from ITC Experiment

system	association constant ($K_b \times 10^5$) (M^{-1})	ΔH^0 (kcal mol^{-1})	$T\Delta S^0$ (kcal mol^{-1})	ΔG^0 (kcal mol^{-1})
		PSF−DNA		
buffer	3.65 ± 0.09	−2.96 ± 0.02	4.59	−7.55 ± 0.02
		PSF−SDS		
buffer	2.14 ± 0.54	−2.77 ± 0.04	4.50	−7.27 ± 0.04
20 mM Na^+	0.23 ± 0.012	−1.99 ± 0.03	3.96	−5.95 ± 0.03
50 mM Na^+	0.05 ± 0.002	−1.34 ± 0.01	3.72	−5.07 ± 0.03
		PSF−DNA complex + SDS		
buffer	0.58 ± 0.04	0.12 ± 0.004	6.62	−6.49 ± 0.01
20 mM Na^+	0.37 ± 0.04	0.10 ± 0.009	6.32	−6.21 ± 0.02
50 mM Na^+	0.27 ± 0.018	0.093 ± 0.006	6.14	−6.04 ± 0.02

however, could not be neglected a priori. In order to understand the contribution of the electrostatic effect on the deintercalation process, we perform the ITC measurements for the PSF−SDS binding and SDS-assisted PSF−DNA deintercalation in presence of Na^+ salt at two different concentrations, viz., 20 and 50 mM. The results are depicted in table 1. As evident from the table, the binding constant of PSF with SDS decreases by orders of magnitude with increasing salt concentration, and the process becomes less favorable (decrease in the overall ΔG^0 value). The observed decrease in the binding affinity can be explained in terms of the shielding of the effective charge of the SDS micellar surface by the salt, which eventually inhibits the otherwise favorable electrostatic binding of the cationic dye PSF. On the other hand, the deintercalation process has been found to be almost indifferent to the addition of salt. Both the binding constant and the overall ΔG^0 values suffer only a marginal decrease, affirming that the electrostatic contribution does not provide a major share in the deintercalation process, as has been predicted by Professor Marcus.[48] Apart from the electrostatic interaction, there is a major role played by the various hydration terms. It is known that the disruption of the water structure around the aromatic moiety and solvation shell of the cationic dye upon intercalation contributes to the positive entropy. There is, however, release of "hydrophobic water", and that is weaker than that re-formed in the bulk.[47] A similar situation prevails in the case of the binding of the ligand with the micelles. However, a net gain in the entropy perhaps lies in the extent of disruption of the solvation shell of the ligand in the two different binding processes; similar to DNA, it is strongly bound to the hydrophobic core of the DNA, while in micelle, its binding is relatively eased. Thus, the entropic contributions from the terms $[PSF{-}DNA]_{hyd}$ and $[PSF{-}micelle]_{hyd}$ are different, and this difference contributes a major share toward the observed ease of the deintercalation process.

Our present investigation is initiated to understand the thermodynamic parameter that drives the deintercalation process. We have used an approximated two-step model, which is a simplification of a rather complicated phenomenon. First, the effect shown by a negatively charged surfactant assembly is surprising because a Coulombic charge repulsion inhibits a close proximity of DNA and SDS micelles. In this regard, it is important to know whether addition of SDS perturbs the structure of the DNA. We carry out CD and absorption spectroscopy measurements of the DNA in the presence of SDS at different concentrations (Figure 6).

It can be observed that the DNA retains its native B form even in the presence of 10 mM SDS, and also the absorption spectra does not suffer any remarkable change upon addition of SDS. This study thus affirms that SDS does not directly interact

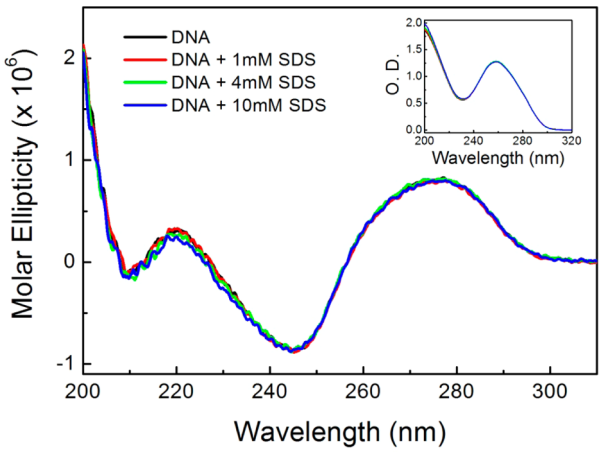

Figure 6. CD spectra of CT DNA in presence and in absence of SDS at different concentrations. Inset shows the corresponding UV-absorbance spectra.

with the DNA. It may be argued that the positive charge of the ligand screens the surface charge of DNA, facilitating the approach of the micelle; however, such an effect is of considerable interest for ligands with multiple charges,[22] and for PSF with a single positive charge, the effect is only marginal. It has been speculated that surfactant molecules bring down the activation energy barrier for the dissociation of the DNA−ligand complex. Perhaps the hydrophobic environment of micelles favors a transit opening of the otherwise compact DNA duplex structure, providing a sink for the exposed hydrophobic moiety of the intercalated ligand driving Process I in a forward direction.[22] The binding of the free drug with the micelle is further catalyzed by the Coulombic attraction. Because Process I serves as the rate-limiting step, hydrophobic contribution offers a key role. It should be understood that the entropy change obtained from the ITC experiment is an overall equilibrium picture which manifests from an interplay of a number of processes occurring in the system including structural reorganization of the DNA due to deintercalation, hydration change, water layer dislocation, water uptake, and probably other effects, and a one-to-one correlation of the entropy change and enthalpy change is not very straightforward. Our study provides a simplified approach toward the understanding of the process, and it will be complementary to study whether the charge type and the overall hydrophobicity of the micelle, base pair sequence in DNA, charge type of the ligand, and so forth contribute toward the overall feasibility of the process, and such a study is underway in our lab.

dx.doi.org/10.1021/jp4091816 | J. Phys. Chem. B 2014, 118, 901−908

CONCLUSIONS

We have studied the energetic parameters of micelle-assisted deintercalation of a model drug PSF from CT DNA. It has been found that binding of PSF to both DNA and SDS micelles offers comparable favorable free energy cost assisted by a negative enthalpy and positive entropy change. The deintercalation process is enthalpy-wise forbidden; however, the process is assisted by a considerable entropic gain. A simplified two-step process reveals that the dissociation of the cationic dye from the DNA interior is assisted by the surfactants, which is also manifested in the corresponding hydration change.

ASSOCIATED CONTENT

Supporting Information

Representative decay transients, time-resolved rotational anisotropy of PSF in SDS micelles, induced CD spectra, and representative ITC profiles (Figures S1–S4). This material is available free of charge via the Internet at http://pubs.acs.org.

AUTHOR INFORMATION

Corresponding Authors

*E-mail: rajib@bose.res.in.

*E-mail: gskumar@iicb.res.in.

Author Contributions

§These authors contributed equally

Notes

The authors declare no competing financial interest.

ACKNOWLEDGMENTS

G.S.K. acknowledges financial support from CSIR network project BIOCERAM. The authors thank the anonymous reviewers for their thoughtful comments.

REFERENCES

(1) Chaires, J. B. Drug–DNA Interactions. *Curr. Opin. Struct. Biol.* **1998**, *8*, 314–320.

(2) Haq, I. Thermodynamics of Drug–DNA Interactions. *Arch. Biochem. Biophys.* **2002**, *403*, 1–15.

(3) Chaires, J. B. Energetics of Drug–DNA Interactions. *Biopolymers* **1997**, *44*, 201–215.

(4) Ren, J.; Jenkins, T. C.; Chaires, J. B. Energetics of DNA Intercalation Reactions. *Biochemistry* **2000**, *39*, 8439–8447.

(5) Chaires, J. B. A Thermodynamic Signature for Drug–DNA Binding Mode. *Arch. Biochem. Biophys.* **2006**, *453*, 26–31.

(6) Dignam, J. D.; Qu, X.; Ren, J.; Chaires, J. B. Daunomycin Binding to Detergent Micelles: A Model System for Evaluating the Hydrophobic Contribution to Drug–DNA Interactions. *J. Phys. Chem. B* **2007**, *111*, 11576–11584.

(7) Berman, H. M. Hydration of DNA: Take 2. *Curr. Opin. Struct. Biol.* **1994**, *4*, 345–350.

(8) Kochoyan, M.; Leroy, J. L. Hydration and Solution Structure of Nucleic Acids. *Curr. Opin. Struct. Biol.* **1995**, *5*, 329–333.

(9) Han, F.; Chalikian, T. V. Hydration Changes Accompanying Nucleic Acid Intercalation Reactions: Volumetric Characterizations. *J. Am. Chem. Soc.* **2003**, *125*, 7219–7229.

(10) Qu, X.; Chaires, J. B. Hydration Changes for DNA Intercalation Reactions. *J. Am. Chem. Soc.* **2001**, *123*, 1–7.

(11) Yu, H.; Ren, J.; Chaires, J. B.; Qu, X. Hydration of Drug–DNA Complexes: Greater Water Uptake for Adriamycin Compared to Daunomycin. *J. Med. Chem.* **2008**, *51*, 5909–5911.

(12) Tanford, C. *The Hydrophobic Effect: Formation of Micellar and Biological Membranes*, 2nd ed.; Wiley Interscience: New York, 1980.

(13) *Anionic Surfactants: Physical Chemistry of Surfactant Action*; Lucassen-Reynders, E. H., Ed.; Marcel Dekker, 1981; Vol. *11*.

(14) Nandi, N.; Bhattacharyya, K.; Bagchi, B. Dielectric Relaxation and Solvation Dynamics of Water in Complex Chemical and Biological Systems. *Chem. Rev.* **2000**, *100*, 2013–2045.

(15) Mitra, R. K.; Sinha, S. S.; Pal, S. K. Temperature Dependent Hydration at Micellar Surface: Activation Energy Barrier Crossing Model Revisited. *J. Phys. Chem. B* **2007**, *111*, 7577–7581.

(16) Pal, S.; Balasubramaian, S.; Bagchi, B. Temperature Dependence of Water Dynamics at an Aqueous Micellar Surface: Atomistic Molecular Dynamics Simulation Studies of a Complex System. *J. Chem. Phys.* **2002**, *117*, 2852–2859.

(17) Bagchi, B.; Jana, B. Solvation Dynamics in Dipolar Liquids. *Chem. Soc. Rev.* **2010**, *39*, 1936–1954.

(18) Rowe, E. S.; Zhang, F.; Leung, T. W.; Parr, J. S.; Guy, P. T. Thermodynamics of Membrane Partitioning for a Series of n-Alcohols Determined by Titration Calorimetry: Role of Hydrophobic Effects. *Biochemistry* **1998**, *37*, 2430–2440.

(19) Tanford, C. Theoretical Models for the Mechanisms of Protein Denaturation. *Adv. Prot. Chem.* **1970**, *24*, 1–95.

(20) Dill, K. A. Dominant Forces in Protein Folding. *Biochemistry* **1990**, *29*, 7133–7155.

(21) Seelig, J.; Ganz, P. Nonclassical Hydrophobic Effect in Membrane Binding Equilibria. *Biochemistry* **1991**, *30*, 9354–9359.

(22) Westerlund, F.; Wilhelmsson, L. M.; Norden, B.; Lincoln, P. Micelle-Sequestered Dissociation of Cationic DNA-Intercalated Drugs: Unexpected Surfactant-Induced Rate Enhancement. *J. Am. Chem. Soc.* **2003**, *125*, 3773–3779.

(23) Wilhelmsson, L. M.; Westerlund, F.; Lincoln, P.; Norden, B. DNA-Binding of Semirigid Binuclear Ruthenium Complex, -[-(11,11′-bidppz)(phen)4Ru2]4+: Extremely Slow Intercalation Kinetics. *J. Am. Chem. Soc.* **2002**, *124*, 12092–12093.

(24) Izumrudov, V. A.; Zhiryakova, M. V.; Goulko, A. A. Ethidium Bromide as a Promising Probe for Studying DNA Interaction with Cationic Amphiphiles and Stability of the Resulting Complexes. *Langmuir* **2002**, *18*, 10348–10356.

(25) Mitra, R. K.; Sinha, S. S.; Pal, S. K. Interactions of Nile Blue with Micelles, Reverse Micelles and a Genomic DNA. *J. Fluoresc.* **2008**, *18*, 423–432.

(26) Mitra, R. K.; Sinha, S. S.; Maiti, S.; Pal, S. K. Sequence Dependent Ultrafast Electron Transfer of Nile Blue in Oligonucleotides. *J. Fluoresc.* **2009**, *19*, 353–361.

(27) Müller, W.; Crothers, D. M. Studies of the Binding of Actinomycin and Related Compounds to DNA. *J. Mol. Biol.* **1968**, *35*, 251–290.

(28) Phillips, D. R.; Greif, P. C.; Boston, R. C. Daunomycin–DNA Dissociation Kinetics. *Mol. Pharmacol.* **1988**, *33*, 225–230.

(29) Das, S.; Kumar, G. S. Molecular Aspects on the Interaction of Phenosafranine to Deoxyribonucleic Acid: Model for Intercalative Drug-DNA Binding. *J. Mol. Struct.* **2008**, *872*, 56–63.

(30) Saha, I.; Hossain, M.; Kumar, G. S. Base Pair Specificity and Energetics of Binding of the Phenazinium Molecules Phenosafranine and Safranine-O to Deoxyribonucleic Acids: A Comparative Study. *Phys. Chem. Chem. Phys.* **2010**, *12*, 12771–12779.

(31) Das, P.; Chakrabarty, A.; Mallick, A.; Chattopadhyay, N. Photophysics of a Cationic Biological Photosensitizer in Anionic Micellar Environments: Combined Effect of Polarity and Rigidity. *J. Phys. Chem. B* **2007**, *111*, 11169–11176.

(32) Saha, I.; Kumar, G. S. Spectroscopic Characterization of the Interaction of Phenosafranin and Safranin O with Double Stranded, Heat Denatured and Single Stranded Calf Thymus DNA. *J. Fluoresc.* **2011**, *21*, 247–255.

(33) Fuguet, E.; Rafols, C.; Roses, M.; Bosch, E. Critical Micelle Concentration of Surfactants in Aqueous Buffered and Unbuffered Systems. *Anal. Chim. Acta* **2005**, *548*, 95–100.

(34) Sarkar, M.; Poddar, S. Studies on the Interaction of Surfactants with Cationic Dye by Absorption Spectroscopy. *J. Colloid Interface Sci.* **2000**, *221*, 181–185.

(35) Pal, P.; Zeng, H.; Durocher, G.; Girard, D.; Giasson, R.; Blanchard, L.; Gaboury, L.; Villeneuve, L. Spectroscopic and Photophysical Properties of Some New Rhodamine Derivatives in

Cationic, Anionic and Neutral Micelles. *J. Photochem. Photobiol., A* **1996**, *98*, 65−72.
(36) Jimenez, R.; Fleming, G. R.; Kumar, P. V.; Maroncelli, M. Femtosecond Solvation Dynamics of Water. *Nature* **1994**, *369*, 471−473.
(37) McMurray, C. T.; Van Holde, K. E. Binding of Ethidium to the Nucleosome Core Particle. 1. Binding and Dissociation Reactions. *Biochemistry* **1991**, *30*, 5631−5643.
(38) McMurray, C. T.; Small, E. W.; Van Holde, K. E. Binding of Ethidium to the Nucleosome Core Particle. 2. Internal and External Binding Modes. *Biochemistry* **1991**, *30*, 5644−5652.
(39) Kelley, S. O.; Barton, J. K. Electron Transfer Between Bases in Double Helical DNA. *Science* **1999**, *283*, 375−381.
(40) Saha, I.; Hossain, M.; Kumar, G. S. Sequence-Selective Binding of Phenazinium Dyes Phenosafranin and Safranin O to Guanine-Cytosine Deoxyribopolynucleotides: Spectroscopic and Thermodynamic Studies. *J. Phys. Chem. B* **2010**, *114*, 15278−15287.
(41) Sarkar, D.; Das, P.; Basak, S.; Chattopadhyay, N. Binding Interaction of Cationic Phenazinium Dyes with Calf Thymus DNA: A Comparative Study. *J. Phys. Chem. B* **2008**, *112*, 9243−9249.
(42) Sidorova, N. Y.; Rau, D. C. The Osmotic Sensitivity of Netropsin Analogue Binding to DNA. *Biopolymers* **1995**, *35*, 377−384.
(43) Parsegian, V. A.; Rand, R. P.; Rau, D. C. Macromolecules and Water: Probing with Osmotic Stress. *Methods Enzymol.* **1995**, *259*, 43−94.
(44) Lepecq, J. B.; Paoletti, C. A Fluorescent Complex Between Ethidium Bromide and Nucleic Acids: Physical−Chemical Characterization. *J. Mol. Biol.* **1967**, *27*, 87−106.
(45) McGhee, J. D.; von Hippel, P. H. Theoretical Aspects of DNA−Protein Interactions: Co-Operative and Non-Co-Operative Binding of Large Ligands to a One-Dimensional Homogeneous Lattice. *J. Mol. Biol.* **1974**, *86*, 469−489.
(46) Frederick, C. A.; Williams, L. D.; Ughetto, G.; Van der Marel, G. A.; Van Boom, J. H.; Rich, A.; Wang, A. H. J. Structural Comparison of Anticancer Drug−DNA Complexes: Adriamycin and Daunomycin. *Biochemistry* **1990**, *29*, 2538−2549.
(47) Becker, H.-C.; Nordén, B. DNA Binding Properties of 2,7-Diazapyrene and Its N-Methylated Cations Studied by Linear and Circular Dichroism Spectroscopy and Calorimetry. *J. Am. Chem. Soc.* **1997**, *119*, 5798−5803.
(48) Marcus, R. A. Micelle-Enhanced Dissociation of a Ru Cation /DNA Complex. *J. Phys. Chem. B* **2005**, *109*, 21419−21424.